Validation of a new cavity ring-down spectrometer for measuring tropospheric gaseous hydrogen chloride

Teles C. Furlani[1], Patrick R. Veres[2], Kathryn E.R. Dawe[3, a], J. Andrew Neuman[2, 4], Steven S. Brown[2,5], Trevor C. VandenBoer[1], Cora J. Young[1]

[1] Department of Chemistry, York University, Toronto, ON, Canada

[2] NOAA Chemical Sciences Laboratory, Boulder, CO, USA

[3] Department of Chemistry, Memorial University of Newfoundland, St. John's, NL, Canada

[4] Cooperative Institute for Research in Environmental Sciences, University of Colorado, Boulder, CO, USA

[5] Department of Chemistry, University of Colorado, Boulder, CO, USA

[a] Now at SEM Ltd., St. John's, NL, Canada

Abstract

Reliable, sensitive, and widely available hydrogen chloride (HCl) measurements are important for understanding oxidation in many regions of the troposphere. We configured a commercial HCl cavity ring-down spectrometer (CRDS) for sampling HCl in the ambient atmosphere and developed validation techniques to characterize the measurement uncertainties. The CRDS makes fast, sensitive, and robust measurements of HCl in a high finesse optical cavity coupled to a laser centered at 5739 cm^{-1}. The accuracy was determined to reside between 5–10%, calculated from laboratory and ambient air intercomparisons with annular denuders. The precision and limit of detection (3σ) in the 0.5 Hz measurement were below 6 pptv and 18 pptv, respectively for a 30

second integration interval in zero air. The response time of this method is primarily characterized by fitting decay curves to a double exponential equation and is impacted by inlet adsorption/desorption, with these surface effects increasing with RH and decreasing with decreasing HCl mixing ratios. The minimum 90% response time was 10 seconds and the equilibrated response time for the tested inlet was 2–6 minutes under the most and least optimal conditions, respectively. An intercomparison with the EPA compendium method for quantification of acidic atmospheric gases showed good agreement, yielding a linear relationship statistically equivalent to unity (slope of 0.97 ± 0.15). The CRDS from this study can detect HCl at atmospherically relevant mixing ratios, often performing comparable or better in sensitivity, selectivity, and response-time from previously reported HCl detection methods.

1. Introduction

Halogenated compounds that participate in catalytic cycles in the atmosphere have major impacts on atmospheric chemistry. Chlorine-containing species have long been known to catalytically destroy stratospheric ozone (Solomon, 1999) and can have similar impacts on tropospheric ozone in polar regions (Simpson et al., 2007, 2015). In particular, early morning oxidation in the troposphere can be influenced heavily by chlorine atoms released by photolabile chlorine species (Osthoff et al., 2008; Thornton et al., 2010; Young et al., 2012, 2014). It is estimated that reactions involving chlorine atoms account for 14–27% of global tropospheric oxidation of abundant volatile organic compounds (VOCs) (Sherwen et al., 2016).

The role of chlorine chemistry in the troposphere remains uncertain in part due to a lack of a complete understanding of the contribution of chlorine reservoir species to the tropospheric chlorine inventory (Osthoff et al., 2008; Young et al., 2014). Sources of inorganic chlorine to the

troposphere are important because many of them are photochemically active (e.g. $ClNO_2$). A near-complete budget of inorganic tropospheric chlorine from aircraft transects of polluted North American continental outflow during the WINTER campaign demonstrated that hydrogen chloride (HCl) makes up 48–62 % of total inorganic chlorine, and approximately 98% of total gaseous inorganic chlorine (Haskins et al., 2018). Troposphere HCl levels are typically between 10 and 1000 parts per trillion by volume (pptv) (e.g. Crisp et al. (2014); Haskins et al. (2018); and Young et al. (2013)). Elevated levels of HCl are typically found near marine environments polluted with NO_x; where reactions involving the chloride in sea spray aerosols can be a major source of chlorine to the troposphere (Crisp et al., 2014; Finlayson-Pitts et al., 1989; Haskins et al., 2018; Wang et al., 2019).

HCl is directly emitted to the atmosphere predominantly from volcanic activity, biomass burning, and industrial sources (Butz et al., 2017; Crisp et al., 2014; Keene et al., 1999). HCl is also produced through heterogeneous acid displacement reactions of strong acids, such as nitric acid, with particulate chloride (pCl^-) (Bondy et al., 2017; Clegg and Brimblecombe, 1985; Gard et al., 1998; Valach, 1967; Wang et al., 2019):

$$HA_{(g, aq)} + MCl_{(aq, s)} \rightarrow MA_{(aq, s)} + HCl_{(g)} \qquad \text{(R1)}$$

where M represents a cation in a chloride salt (often sodium). Elevated levels of chlorine atoms may also be present in both indoor and outdoor environments due to the emission of photolabile reactive chlorine compounds (Dawe et al., 2019; Mattila et al., 2020; Osthoff et al., 2008; Young et al., 2014, 2019).

$$XCl_{(g)} + h\upsilon \rightarrow Cl\cdot_{(g)} + X\cdot_{(g)} \qquad \text{(R2)}$$
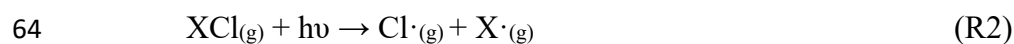
Secondary production of HCl predominantly occurs *via* the reaction of chlorine atoms with methane or VOCs by hydrogen abstraction:

$$Cl\cdot_{(g)} + CH_{4(g)} \rightarrow HCl_{(g)} + \cdot CH_{3(g)} \hspace{2cm} (R3)$$

$$Cl\cdot_{(g)} + RH_{(g)} \rightarrow HCl_{(g)} + R\cdot_{(g)} \hspace{2cm} (R4)$$
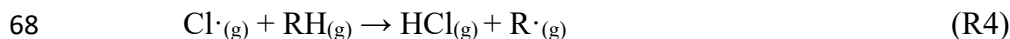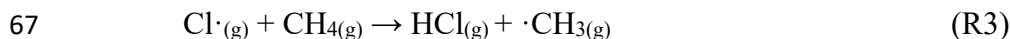
The loss of gas-phase HCl occurs predominantly through wet or dry deposition which are terminal sinks for tropospheric chlorine (Wang et al., 2019), with minor loss by reaction with the hydroxyl radical (OH) to re-form chlorine atoms:

$$HCl_{(g)} + OH\cdot_{(g)} \rightarrow Cl\cdot_{(g)} + H_2O_{(g)} \hspace{2cm} (R5)$$
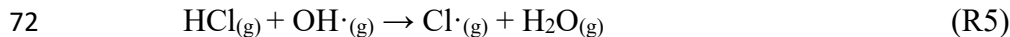
The balance between loss and formation of chlorine atoms from HCl is highly dependent on factors such as the presence of pCl$^-$, NO$_x$ (NO$_x$=NO+NO$_2$), and HCl deposition rate (Finlayson-Pitts et al., 1989; Roberts et al., 2008).

Measuring HCl in the gas phase is challenging as it readily adsorbs to surfaces. Methods for atmospheric HCl detection must be sensitive, robust, and selective and address HCl interactions with instrument surfaces. Mass spectrometry based measurement techniques have been developed for the detection of HCl in both the stratosphere and troposphere (e.g. Huey et al. (Huey et al., 1996) and Marcy et al. (2004)). Other methods include scrubbing ambient air using an annular denuder and/or a tandem mist chambers to collect HCl, followed by offline analysis such as ion chromatography (IC) (Keene et al., 2007, 2009; United States Environmental Protection Agency, 1999; Young et al., 2013). Online detection methods such as chemical ionization time of flight mass spectrometry (CI-ToF-MS) (Crisp et al., 2014), negative ion proton transfer chemical ionization mass spectrometry (NI-PT-CIMS) (Veres et al., 2008), and negative mode atmospheric pressure chemical ionization coupled to triple quadrupole mass spectrometry (APCI-MS-MS)

87 (Karellas et al., 2003) have been shown to be reliable and sensitive methods for HCl detection.

88 Limitations to these existing HCl measurement techniques include some or all of the following;

89 detection limits that are not suitable for the low level of HCl in the troposphere, slow time response,

90 lack of portability, and calibration challenges. Spectroscopic techniques offer distinct advantages

91 over some previous methods. Spectroscopic techniques for measuring atmospheric HCl reported

92 by Hagen et al. (2014) and Wilkerson et al. (2021) have shown the precedent for fast time response,

93 as well as sensitive, selective, and robust detection. The portability and fast time response for

94 instruments is of great importance for spatial resolution and is therefore a key factor for field

95 deployment.

96 Measurements of HCl are typically calibrated using HCl from permeation devices and or

97 standards in compressed gas cylinders. Method validation for HCl measurements are rare, but can

98 reduce these uncertainties (Hagen et al., 2014; Wilkerson et al., 2021). In this paper we

99 demonstrate the versatility and validation of a new commercial cavity ring-down spectrometer

100 (CRDS) for in-situ atmospheric gas phase HCl measurements. First, we compare this CRDS with

101 existing HCl measurement techniques through lab and field intercomparisons. Finally, we describe

102 and characterize surface effects and recommend inlet configurations for best practices when

103 conducting ambient sampling.

2. Materials and experimental methods
104

2.1 Chemicals
105

106 Reagent grade hydrochloric acid (HCl, 12 M) was used in permeation device construction

107 (see Section 2.3). Potassium hydroxide (KOH) pellets were used to create scrubbing solution for

108 permeation device gas collection. Commercially available reagents were from Sigma-Aldrich

109 (Oakville, Ontario, Canada) and Ultra zero air (grade 5.0) gases were from Praxair (Toronto,

110   Ontario, Canada). Experiments used deionized water generated by a Barnstead Infinity Ultrapure

111   Water System (Thermo Fisher Scientific, Waltham, Massachusetts, USA; $18.2\,\text{M}\Omega\,\text{cm}^{-1}$). Annular

112   denuder coating solution was prepared with reagent grade (>95.5%) sodium carbonate (Sigma-

113   Aldrich, St. Louis, Missouri, USA), reagent grade glycerol (Sigma-Aldrich, St. Louis, Missouri,

114   USA), HPLC grade methanol (Fisher Chemicals, Ottawa, Ontario, Canada), and $18.2\,\text{M}\Omega\,\text{cm}^{-1}$

115   deionized water. Eluent for annular denuder IC analysis was prepared from sodium hydroxide

116   solution (NaOH, 50% w/w, Thermo Fisher Scientific, Sunnyvale, California, USA). IC calibration

117   standards were prepared through serial dilution of a mixed anion standard concentrate (Thermo

118   Fisher Scientific, Dionex Seven-Anion II, P/N: 057590). Nitrogen (grade 4.8).

119   **2.2. Cavity ring-down spectrometer (CRDS)**

120   The Picarro G2108 Hydrogen Chloride Gas Analyzer system was used for all analyses.

121   The basic operating principles of this CRDS are similar to analogous Picarro greenhouse gas

122   instruments that have been described in detail by Crosson et. al (2008). The CRDS consists of a

123   tunable laser, a wavelength monitor, and a heated optical cavity (80 °C). All the components of

124   this analyzer and internal stainless-steel fittings are contained within a heat-regulated metal case

125   maintained at 45 °C. The laser radiation (1742 nm, 5739 cm^{-1}) is directed by a fiber optic cable to

126   the wavelength monitor and optical cavity. The first overtone (2-0 absorption band) of HCl is

127   easily discernable from other absorbing species (e.g. H_2O, CH_4), has a relatively high intensity

128   compared to the fundamental absorption transition, and is accessible to near-infrared (IR) diode

129   laser light sources. The optical cavity is fitted with three highly reflective dielectric-coated fused

130   silica mirrors (R > 99.995%, ring down time constant of 53 μsec, equivalent to a path length of 16

131   km) oriented in an acute triangular arrangement supported by an invar housing. The reflectivity of

132   the mirrors is measured from the laser signal loss in an analyte-free optical cavity under inert gas

133 flow. The CRDS flow rate is 2 L min^{-1} and the cavity is held at a reduced pressure of 18.70 ± 0.02

134 kPa (140 Torr) thermostated to $80.000 \pm 0.005°C$. One mirror is mounted on a piezoelectric

135 actuator to achieve optical resonance between the laser frequency and the longitudinal modes of

136 the cavity. The laser is shut off rapidly (< 1 μsec) once resonance is achieved. A photodetector

137 monitors the decay of the photons exiting the cavity through another mirror. Custom electronics

138 digitize the signal for fitting of an exponential decay; the time constant of the decay, τ, is converted

139 to absorbance, α, using the expression

140 $$\alpha = 1 \: / \: c\tau - 1 \: / \: c\tau_0 \quad \text{E1}$$

141 where c is the speed of light. The instrument measures 30 specific frequencies within ~1 cm^{-1}

142 centered at 5739 cm^{-1} to fit the absorption spectra of trace species in this region (see Figure S2).

143 HCl, H_2O, and CH_4 mixing ratios are reported every 2 seconds, though the true time response of

144 the measurement method is limited by surface effects (see Section 3.4). Gaseous inorganic chlorine

145 reservoir species (e.g. $ClNO_2$) cannot thermally dissociated under the cavity (80 °C) conditions

146 (Thaler et al., 2011). The instrument zero measurement drift is reduced by a high precision

147 distributed feedback laser centered at 5739.2625 cm^{-1} coupled with a custom-designed wavelength

148 monitor to determine the frequency axis of each spectrogram. To mitigate particulate matter optical

149 extinction and surface deposition on the high reflectivity mirrors, two high efficiency particulate

150 air (HEPA) filters are placed upstream of the cavity, contained within the 45 °C heat-regulated

151 compartment.

152 **2.3 In-house HCl permeation device validation**

153 The in-house assembly of HCl permeation devices (PDs) is described in detail in Lao et al.

154 (2020). Briefly, 200 μL of 12 M aqueous HCl solution was pipetted into a 7.62 cm perfluoroalkoxy

155 (PFA) tube (3 mm i.d. with 1 mm thickness) plugged at both ends with porous

156 polytetrafluoroethylene (PTFE) (1 cm length by 3.17 mm o.d.). The polymers allow a consistent

157 mass of HCl to permeate at a given temperature and pressure. An aluminum block that was

158 temperature-controlled using a cartridge heater (Omega^{TM}; CIR-2081/120V, Saint-Eustache, QC,

159 Canada) housed the PD and was regulated to 60.0 ± 0.1 °C by a process controller. Dry N_2 flowed

160 through a PFA tube (1.27 cm o.d.) in the block, containing the PD. Stable flows of 49 ± 2 standard

161 cubic centimeters per minute (sccm) through the oven were maintained with a 50 μm diameter

162 critical orifice (Lenox laser, Glen Arm, Maryland, USA, 15 psi; SS-4-VCR-2-50). Flows were

163 measured using a DryCal Definer 220 (Mesa Labs, Lakewood, Colorado, USA). The mass

164 emission rate of HCl from the PD was quantified by scrubbing into a 25 mL glass impinger

165 containing 1 mM KOH over 24 h followed by analysis using IC with conductivity detection (CD).

166 Mass emission rates for the PD were determined as 140 ± 18 ng min^{-1} (n=3, $\pm 1\sigma$) at 60 °C.

2.4 Laboratory intercomparison

168 A laboratory intercomparison between the CRDS and offline-measured HCl scrubbed into

169 a basic solution of 100 mM KOH by delivering gaseous HCl from the permeation device to the

170 sampling systems. The 140 ng min^{-1} of HCl in dry N_2 from the PD was mixed into a zero air

171 dilution flow of 2.1 to 8.0 L min^{-1}, to provide standard addition HCl mixing ratios that ranged from

172 12 to 45 ppbv.

173 The dilution flow was maintained using a 10 L min^{-1} mass flow controller (GM50A, MKS

174 instruments, Andover, Massachusetts, USA). All inlet lines and fittings were kept at ambient

175 temperature (~25 °C) and were made of PFA unless stated otherwise. The inlet mixing line

176 between the PD emissions and the humidified dilution flow was 3.17 mm i.d. and 45 cm in length.

177 Residence times for HCl in the sampling line ranged from 0.02 to 0.08 seconds. To vary relative

178 humidity (RH), a controlled flow of zero air was directed into a glass impinger at room temperature

179 containing deionized water to yield a water-saturated air stream. The humidified flow was passed

180 through a 2 µm Teflon filter (TISCH scientific, North Bend, Ohio, USA) in a PFA holder to

181 prevent any aqueous droplets from entering the experimental lines. The RH was set by mixing

182 with dry zero air to generate 0, 20, 50, and 80 % RH values.

2.5 Ambient intercomparison

184 An ambient intercomparison was undertaken by measuring outdoor air with the CRDS in

185 parallel with sodium carbonate-coated annular denuders. A total of 11 denuder samples were

186 collected alongside continuous CRDS observations, each for approximately 24 hours between 4–

187 11 April 2019. The measurement site was the Air Quality Research Station, located on the roof of

188 the Petrie Science and Engineering Building at York University in Toronto, Ontario, Canada

189 (43.7738° N, 79.5071° W, 220 m above sea level). All indoor inlet lines and fittings were kept at

190 room temperature while the outdoor temperature ranged from -2 to 14 °C. All inlet lines and

191 fittings were made of PFA unless stated otherwise. A full schematic of the sampling apparatus

192 indicating the separation between the outdoor and indoor inlet positions is provided in Figure S5.

193 A 22 L min^{-1} sampling flow was pulled through a URG Teflon Coated Aluminum Cyclone (URG

194 Corporation, Chapel Hill, North Carolina, USA) with a 2.5 µm cut-off for particulate matter. The

195 inlet lines were such that each sampling setup collected HCl at equal residence time to ensure

196 equivalent wall losses of HCl. The shared inlet line was 4.65 m in length and had an i.d. of 4.76

197 mm. The flow was split between the 1.5 m denuder sampling line (20 L min^{-1}) and the 0.15 m

198 CRDS sampling line (2 L min^{-1}), yielding a 0.375 sec residence time for both methods. The

199 denuder line flow was equally divided into two multichannel etched glass annular denuders (URG

200 Corporation, Chapel Hill, North Carolina, USA, 4 channel, 242 mm length, URG-2000-30x242-

201 4CSS) at 10 L min^{-1}. The denuders collected HCl in parallel to each other with flows controlled

202   using two separate 10 L min^{-1} mass flow controllers (GM50A, MKS instruments). Denuders were

203   coated with a solution of 2% w/w sodium carbonate and 0.1% w/w glycerol in a solution of 1:1

204   methanol:water. A 15 mL aliquot of coating solution was dispensed into a denuder and two

205   polypropylene caps affixed. The sealed denuders were inverted and rotated for a few minutes to

206   ensure an even coating. The excess coating solution was decanted, and the denuder was dried for

207   15 min with 2 L min^{-1} of zero air. After sampling, denuders were extracted with 2 aliquots of 5.00

208   mL deionized water, following the same sealing and inversion procedure, for a total extraction

209   volume of 10.00 mL. Extracts were collected into a 15 mL polypropylene tube for storage at 4 °C

210   until analysis. Instances of flagged instrument errors in the CRDS data during ambient

211   observations were removed as standard practice in quality control procedures (see Figure S3). The

212   loss of observational data during such periods corresponds to a negative bias. The CRDS data loss

213   during a given denuder sampling period was included in setting the overall measurement error

214   when intercomparing measurements.

215   **2.6 Ion chromatography analysis**

216   Samples collected into an impinger from the HCl PD were analyzed as the chloride anion

217   by IC-CD using an ICS-2100 (Thermo Fisher Scientific, Sunnyvale, California, USA) according

218   to the method described in Place et al. (Place et al., 2018). Annular denuder extracts were analyzed

219   by IC-CD using an ICS-6000 (Thermo Fisher Scientific, Sunnyvale, California, USA). Details of

220   both separation methods can be found in the SI. Chloride was quantified using external calibration

221   with a 5-point calibration curve. Two check standards, located at the high and low ends of the

222   working range, were used to evaluate the accuracy of quantification.

223   **3. Results and discussion**

224   **3.1 Suitability for atmospheric measurements**

225   The selectivity of this CRDS analyzer arises from monitoring a high-intensity spectral line

226   (5739.2625 cm^{-1}). The absorption used by this instrument is suitable for HCl measurements in the

227   ambient atmosphere because abundant atmospheric gaseous species such as CO, CO_2, NO_x, and

228   N_2O (Gordon et al., 2017; Kochanov et al., 2019) do not have major absorption features in the

229   same region. Absorption features of H_2O and CH_4 in this spectral region are part of the fitting

230   parameters used to determine number densities of HCl, as described in Section 2.2. Most organic

231   and inorganic compounds commonly found at trace levels in the atmosphere do not absorb strongly

232   in this region (Gordon et al., 2017; Kochanov et al., 2019). For these compounds to interfere with

233   the CRDS measurement, their mixing ratios would need to be very high (>10s of parts per million

234   by volume, ppmv). Under conditions where the peak shape is compromised by the presence of

235   interfering absorbing species or instrument instabilities (e.g. cavity pressure fluctuations), the

236   instrument fitting is interrupted and the "bad" data is flagged, thereby allowing simple quality

237   control (see Figure S3).

238   The limit of detection (LOD) of the CRDS analyzer is suitable for expected HCl levels in

239   the atmosphere. Instrument LODs were calculated as three times the Allan-Werle deviation (Figure

240   1, Hagen et al., 2014) when overflowing a 15 cm inlet (3.17 mm i.d.) with zero air directed into

241   the CRDS for ~10 hours. The LODs determined in the CRDS measurements for 2 second, 30

242   second, 5 minute, and 1 hour integration times were 66, 18, 5, and 2 pptv, respectively. Similarly,

243   precision was determined from the Allan-Werle deviation in the blank over the same 10 hours of

244   zero air sampling. Precision in a 2 second, 30 second, 5 minute, and 1 hour integration time was

245   22, 6, 2, and 0.8 pptv, respectively.

246
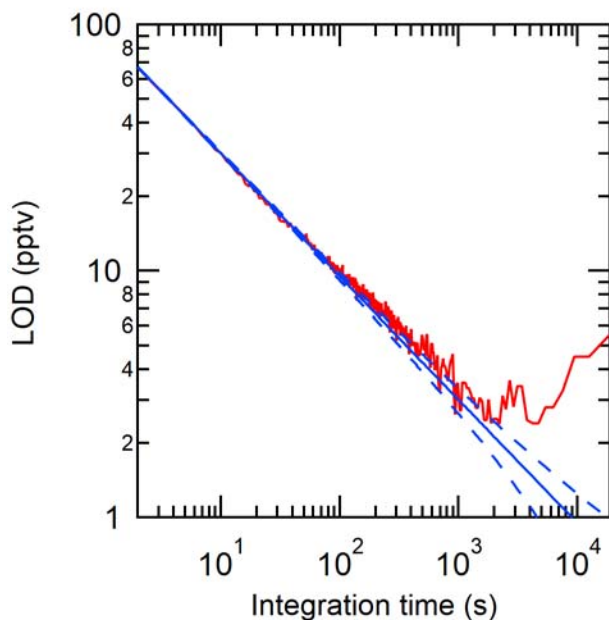
Figure 1. Allan-Werle deviation (3σ) in the optical cavity purged with zero-air (red line) shown with the ideal deviation (no drift, solid blue line) and associated error in the deviation (dashed blue line).

3.2 Instrument performance

This CRDS has many advantages compared to methods previously used to measure HCl in the ambient atmosphere (Table 1). The LOD and precision of the instrument is comparable to prior high time-resolution methods, allowing changes in HCl mixing ratio of a few pptv to be measured. The accuracy/uncertainty is the hardest to compare due to the differences in assessment. A particular challenge is that other methods require external calibrations to determine accuracy and a stable, accurately calibrated HCl source at atmospherically relevant mixing ratios is challenging to obtain (Lao et al., 2020; MacInnis et al., 2016). In contrast, spectroscopic techniques offer a distinct advantage as they are absolute measurements and accuracy determinations rely on propagating uncertainty in the measured parameters (i.e. wavelength and the time constant τ). In the absence of determining accuracy of the CRDS from its operating parameters we use the deviations in our intercomparisons to estimate the accuracy of the full system, i.e. the instrument and ambient sampling inlet combined. We assess the total method uncertainty using

262   intercomparisons with the gold standard for atmospheric acid detection (EPA Compendium

263   method IO-4.2, United States Environmental Protection Agency (United States Environmental

264   Protection Agency, 1999)) due to the greater uncertainty when considering the potential total

265   system error from the sorption/desorption to all sampling surfaces (i.e., instrument and inlet). We

266   measured that the accuracy of the analyzer ranges from 5 to 15%. This is a conservative range

267   based on the methods we used to validate the instrument, which is further described in Section 3.3.

268   The response time of the CRDS used in this work is fast compared to most measurements; the

269   limitation for all online-line methods compared in Table 1 is not the measurement frequency, but

270   rather the time required for HCl to adsorb and desorb from the inlet to the sample stream, which

271   is discussed further in Section 3.5. Lastly, instrument size and power consumption of this CRDS

272   are much lower than many other techniques and are major advantages when considering use in the

273   field, particularly for mobile platforms.

274   **Table 1.** Performance characteristics of CRDS HCl analyzer compared to previously reported

275   methods.

Instrument	LOD	Accuracy/ Uncertainty	Precision	Measurement frequency	Instrument Size	Power Consumption	Reference
Near-IR CRDS	<18 pptv[a] (30 sec)	5–15%	6 pptv (30 sec)	2 s[e]	31.75 kg 43.2 x 17.9 x 44.6 cm	110 W (analyzer) 75 W (pump)	This study
Near-IR CRDS	60 pptv[a] (1 min)	<10%	20 pptv (1 min)	<15 s	NR	NR	(Hagen et al., 2014)
Off-axis integrated cavity output spectrometer (OA-ICOS)	78 pptv (30 sec)	<11%	26 pptv (30 sec)	1 s	NR	NR	(Wilkerson et al., 2021)
Aircraft laser infrared absorption spectrometer	33 pptv[b]	10 %	0.1 ppbv (30 sec)	<30 s	72 kg	NR	(Voss et al., 2001; Webster et al., 1994)

Quartz-enhanced photoacoustic spectroscopy (QEPAS)	550 ppbv[a]	NR	526 ppbv	NR	NR	NR	(Ma et al., 2016)
Acetate CI-ToF-MS	97 pptv[a]	30%	32.3 pptv	<1 s	59 x 42 x 83 cm	<2000 W peak	(Crisp et al., 2014)
Iodide CI-HR-ToF-MS	30 pptv[a] (30 sec)	30%	10 pptv (30 sec)	0.22 s	~ 59 x 42 x 83 cm	<2000 W peak	(Lee et al., 2018)
Sulfur pentaflouride ion trap CIMS	66 pptv[a]	10%	22 pptv	1.6 s	NR	NR	(Jurkat et al., 2010)
APCI-MS-MS	335 pptv[a]	NR	NR	5 s	NR	< 17.5 kW	(Karellas et al., 2003)
Tandem mist chamber and IC-CD	48 pptv[c]	<25 %	24 pptv[c]	2 h	NR	NR	(Keene et al., 2007, 2009)
Annular denuder and IC-CD	6.9–42 pptv[d]	10%	NR	Hours–Days	>10 kg	400 W (Sampling equipment only)	This study

276 a: 3σ, b: predicted assuming a minimum detectable line-center absorption of 1×10^{-5} can be achieved in 30 s, c:

277 precision (σ) determined from averaged paired measurements in 2 h samples on IC-CD and LOD was calculated at

278 2σ, d: 3σ calculated range for a 24-hour sampling time from three denuder method blanks, e: instrument data reporting

279 frequency. The true measurement frequency will also be affected by surface effects, as described in section 3.4, and

280 NR: not reported.

3.3 Laboratory and ambient intercomparison

282
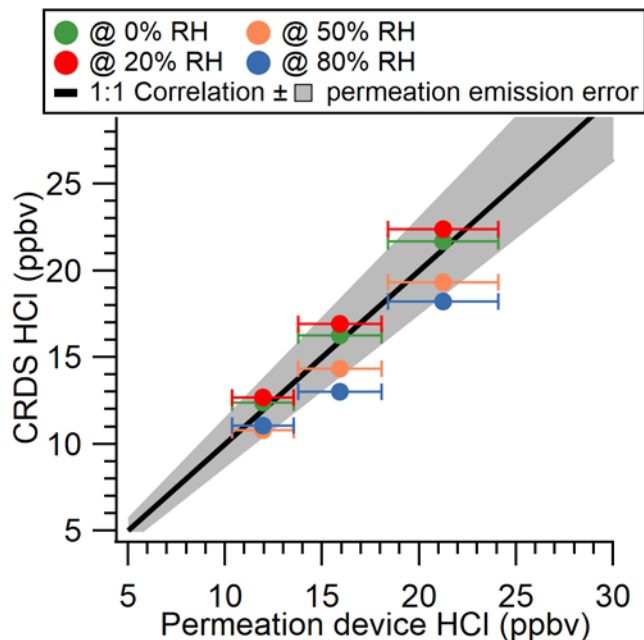
Figure 2. Comparison of CRDS HCl measurements and output from an HCl permeation device over a range of RHs. Error bars in the x direction represent propagated IC measurement error, while error bars in the y direction represent the standard deviation of online sampling plateau for each mixing ratio (low magnitudes mean these error bars do not extend beyond the points). A 1:1 correlation (solid black line) is shown with the uncertainty in the permeation device emission rate (shaded grey area).

We compared the CRDS analyzer-measured HCl with the gas standard mixing ratios provided by an IC-certified PD under dry conditions and observed a close to 1:1 correlation. We explored 5 mixing ratios 12, 16, 21, 32, and 45 ppbv. These levels are higher than have been observed in the ambient atmosphere but demonstrate good single response linearity. When the HCl gas entrained in flows of higher RH ($\geq$ 50 %) a negative bias was observed, although the measurements generally remained within the quantified error in the PD output. Negative bias from the provided HCl mixing ratios at 50 % and 80 % RH were 9.6 % and 14.9 %, respectively. As described above, there is no spectroscopic water absorption interference in the HCl measurement indicating that water increased HCl losses to gas handling surfaces for experiments conducted in humidified air. Inlet surface effects are well established for gaseous strong acids and bases, as these compounds readily sorb at interfaces (e.g. Eisele and Tanner (1993), Kim et al. (2008),

299 Neuman et al. (1999), Pszenny et al. (1993), Roscioli et al. (2016)). The comparison presented

300 here is a best-case scenario because the sampled mixing ratios were much greater than expected in

301 the ambient atmosphere, and therefore less likely to be impacted by surface effects. Surface effects

302 under humid conditions necessitated the mitigation and quantification efforts described further in

303 Section 3.5. To practically validate the CRDS under real-world conditions, an ambient

304 intercomparison was performed over a period of 7 days (4–11 April 2019).

305
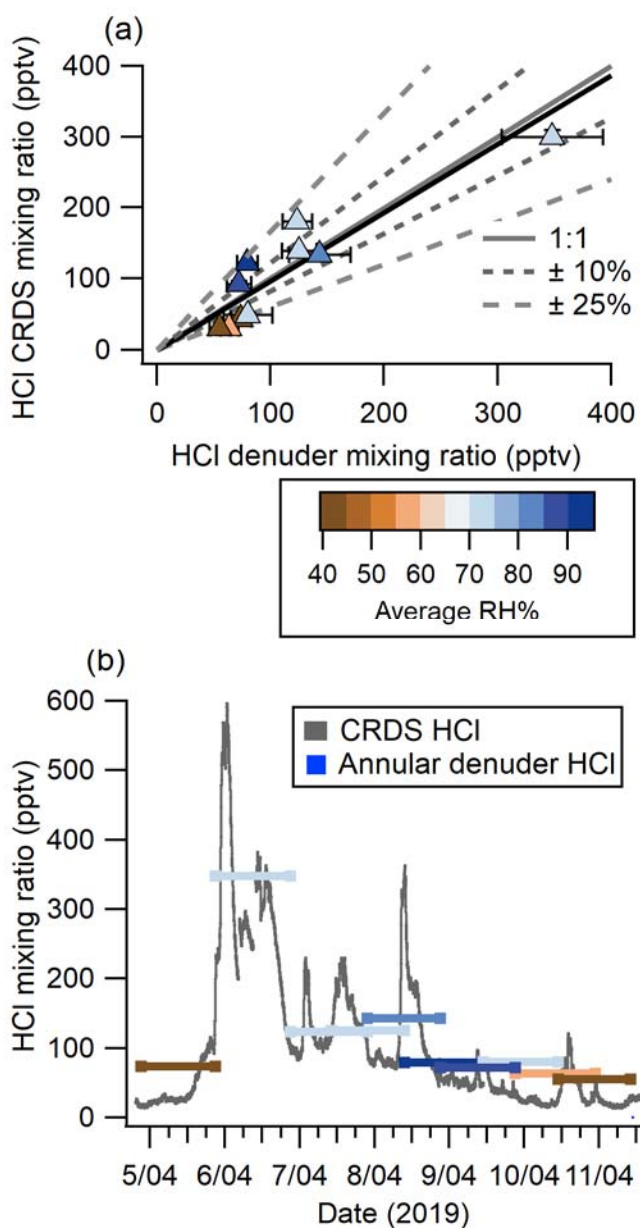
Figure 3. (a) Comparison of HCl measured 4–11 April 2019 using annular denuders and CRDS (averaged to the collection time of denuders). Denuder error bars are derived from the error in the IC calibration, standard deviation of method blanks, and extraction recovery. CRDS measurement errors are the precision in a single measurement combined with data loss for flagged instrument errors. Also shown are a 1:1 correlation line (solid grey), 10 % (short grey dash) and 25 % (long grey dash) deviation from 1:1, and the orthogonal distance regression (solid black). Points are coloured by the average RH during sampling. (b) Continuous HCl mixing ratio timeseries by CRDS overlaid with averaged 24-hour denuder measurement analyzed by IC with lines coloured according to the average RH during sampling.

Online HCl detection by CRDS showed good agreement with HCl mixing ratios quantified from ten annular denuder extracts collected according to EPA Compendium method IO-4.2 (United States Environmental Protection Agency, 1999), which is a standard offline method for quantitation of acidic atmospheric gases (see Figure 3a). Measurements from the 2 instruments were linearly related with a slope of 0.97 ± 0.15, as determined by orthogonal least distance regression, with a y-intercept of -0.001 ± 0.021. Half of the measurements are within 10 % of a 1:1 correlation and the remaining half fall within 25 %. To further validate the comparison a linear correlation coefficient (see Figure S7) of 0.93 ± 0.14 was determined for the two methods and shows good agreement with the orthogonal least distance regression. Changes in RH had no systematic bias on the correlation. Our intercomparison indicates that CRDS measures HCl with comparable results to those obtained by carbonate-coated annular denuders. While the latter requires offline analysis, the CRDS has the additional benefit of continuous high time resolution measurements at 0.5 Hz and dramatically better precision.

Although average HCl measurements between the CRDS and denuders agreed well, much of the useful temporal variability were lost in the time-integrated denuder data (see Figure 3b). For example, from 19:00 April 5 to 01:00 April 6 the CRDS measured mixing ratios between 91 and

331   598 pptv. This rapid change of mixing ratios is not captured by the 24-hour average denuder-

332   measured mixing ratio of 348 pptv. The fast time response of the CRDS also captured other rapidly

333   changing HCl features such as the peak observed on between 00:00–06:00 on April 7. The 6-hour

334   event started at 80 pptv and increased at a rate of 1.2 pptv min^{-1} to 230 pptv over ~120 minutes,

335   followed by a decrease at a rate of 0.5 pptv min^{-1} for ~240 minutes to 98 pptv. The fast time

336   response of the CRDS on the order of minutes is crucial when applying the technique to the real

337   atmosphere for the purpose of fully constraining the sources and sinks for HCl, for which many

338   precursors have similar lifetimes, and ultimately improve our understanding of the Cl budget

339   (Crisp et al., 2014).

340   Results from the laboratory and ambient intercomparisons were used to determine the

341   accuracy of the HCl analyzer as 5 to 15 %. The lower bound of uncertainty (5 %) was determined

342   from the laboratory intercomparison under the optimal dry conditions (Figure 2). The upper bound

343   of uncertainty (15 %) was consistent across the laboratory intercomparison under the highest RH

344   (80%) conditions tested (Figure 2) and the standard deviation of the orthogonal distance regression

345   slope from the ambient intercomparison (Figure 3a).

346   **3.4 Sampling line and instrument response time assessment**

347   We have thus far demonstrated the efficacy of the CRDS for accurately analyzing gas

348   standards and ambient HCl. However, the potential for sampling losses or desorption sources of

349   surface-active gases that could affect the quality of such measurements is ubiquitous, and the study

350   of these effects are well established (Crisp et al., 2014; Ellis et al., 2010; Pollack et al., 2019;

351   Roscioli et al., 2016). This makes quantification a challenge as there are typically long

352   equilibration times associated with signal stabilization. Long equilibrations make fast time

353   response detection difficult without first characterizing line sorption and desorption, followed by

354   making inlet modifications to minimize losses (Deming et al., 2019; Ellis et al., 2010; Pagonis et

355   al., 2017). To ensure accurate field measurements of HCl, a characterization of the magnitude of

356   HCl loss and desorption during sampling was made. The response time of an instrument to a rapid

357   change in HCl can be calculated by both the time it takes for the measurement to go from zero to

358   100 % of the HCl quantity being delivered, as well as the time it takes to return from the HCl

359   quantity being delivered back to zero.

360   Inlet and instrument surface effects for surface active gases such as HCl can be

361   characterized by fitting decay curves to a double exponential (Ellis et al., 2010; Moravek et al.,

362   2019; Pollack et al., 2019; Zahniser et al., 1995);

363    $$y = y_0 + A_1 e^{\left(-\frac{t-t_0}{\tau_1}\right)} + A_2 e^{\left(-\frac{t-t_0}{\tau_2}\right)} \quad \text{E2}$$

364

365   Where y is the mixing ratio of HCl, y_0 is the mixing ratio at the end of the decay, A_1 and A_2 are

366   proportionality coefficients that determine how much the decay is governed by τ_1 and τ_2

367   respectively, t is the time elapsed, and t_0 is the initial time. The first time constant (τ_1) represents

368   air exchange within the instrument, while the second (τ_2) is the surface interaction equilibrium

369   time between HCl adsorbed to surfaces and the overlying airstream mixing ratio. The only term in

370   this equation that can be optimized for the CRDS is τ_2, which can be reduced by decreasing the

371   amount of time HCl interacts with inlet surfaces. The sampling flow rate and cavity temperatures

372   are constant for the commercial software and not adjustable, therefore changing the value of τ_1

373   was not explored in this study. In most reports τ_1 represents the largest change in signal and

374   represents instrument response time. For example, Whitehead et al. (2008) found that τ_1 values

375   governed >75% (i.e. A_1) of changes in measured NH_3. For the CRDS, measured values of τ_1 were

376   between 5 and 10 seconds under all conditions and could be improved with a faster inlet flowrate

377   for the CRDS to subsample from.

378   An additional set of experiments was undertaken in which a 24 ppbv HCl standard was

379   sampled while varying RH from 0 to 33% (Figure 4). The effect of RH on the response time of the

380   CRDS was measured using a method similar to that described in Section 2.4. The HCl standard

381   gas was sampled over three 10 min pulses at each RH ($\pm$ 2%). The HCl standard was introduced

382   into a 3.17 mm i.d. PFA tube and 10 cm long inlet line. Data was background corrected to levels

383   measured prior to the standard addition and the signal was normalized to the HCl enhancement

384   during the final 10 seconds of each HCl pulse. Due to a lack of inlet characterization for systems

385   measuring HCl, we compare our decay constants to literature values for compounds with similar

386   surface-active properties (e.g. HNO_3 and NH_3). The instrument exchange rate (τ_1) values for

387   spectroscopic methods measuring HNO_3 and NH_3 are generally faster than our measured values

388   for HCl. However, it should be noted that measurements of τ_1 reflect differences in sampling flow

389   rates and internal volume and are likely affected by the internal filters present in the HCl CRDS.

390   Typically, τ_1 was <2 seconds (Ellis et al., 2010; Pollack et al., 2019; Roscioli et al., 2016), but

391   could be as high as 4.5 seconds for larger pulses (1 ppmv) of analyte (Roscioli et al., 2016). We

392   observed a highly variable surface interaction equilibrium time constant (τ_2), with values ranging

393   between 97 and 350 seconds. Reported values of τ_2 for other surface-active gases are similarly

394   variable, with values <50 seconds for heated short clean inlets (Ellis et al., 2010; Pollack et al.,

395   2019; Roscioli et al., 2016), and ~300 seconds for a contaminated inlet measuring NH_3 (Pollack et

396   al., 2019). Major differences in the surface area between our instrument and the instruments to

397   which we compare are likely to cause τ_2 differences. Our method employs the use of three filters

398   that increase the gas to surface interactions, and therefore increase our equilibrated response time

399   τ_2..

400
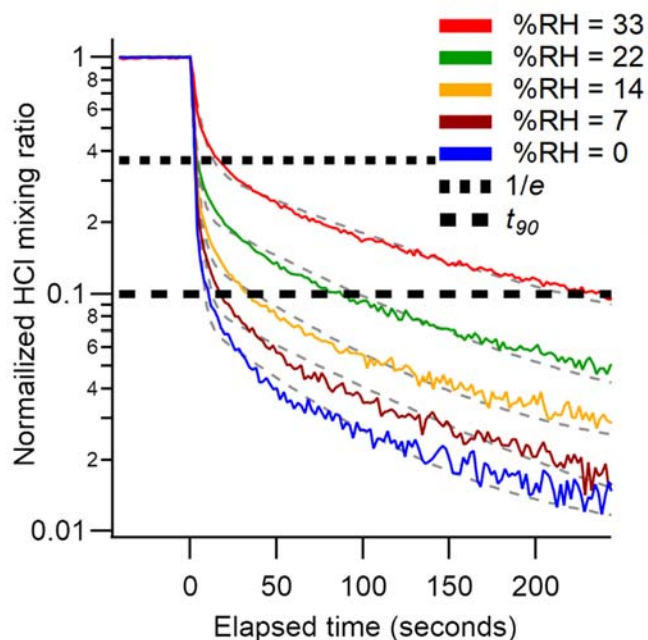
Figure 4. Background corrected and normalized signal decay curves observed for pulsed HCl (24 ppbv)
performed at various RHs. Dashed grey lines represent a double exponential fit to the average of three
cycles at each water mixing ratio. The short and long dashed black lines indicate 37 % (1/e) and 90 % (t_{90})
decrease from the initial signal, respectively.

405

406   Another method for quantifying response time is by calculating the e-folding (1/e) signal

407   loss with respect to time. Calculated e-folding response times demonstrated the fast exchange

408   within the system with values comparable to τ_1. Similarly, a signal decrease of 90% (t_{90}) illustrates

409   the total decay of the sampling line. Using e-folding response time and t_{90} offers a better visual

410   understanding of the relative roles for instrument and inlet responses and the impacts of increasing

411   RH. We summarize the double exponential decay constants, e-folding response time, and t_{90} for

412   the rise and decay of HCl mixing ratios from pulses delivered to the instrument in Table 2 and SI

413   tables 1–4. Increasing the RH increases the response time of the inlet (Figure 4). At the highest

414   experimental RH (33 %), τ_2 is increased by almost a factor of two compared to dry conditions,

415 from seconds to minutes. At lower mixing ratios the higher RH increased the response times to a

416 greater extent (Table 2 and Tables S1–S4). The increased response time at high ambient RH would

417 not compromise stationary measurements in which HCl mixing ratios changed on time scales of

418 minutes to hours but would not capture more rapid changes. The largest impact on CRDS time

419 response likely comes from unavoidable effects of partitioning on the large surface area of the

420 HEPA filters located before the optical cavity. Minimizing inlet effects for the CRDS where

421 observation of HCl mixing ratio changes over <1 min is required (e.g. aircraft or mobile

422 measurements) are most important. The wall interactions of HCl can be reduced by increasing the

423 inlet flow rate and/or decreasing the tubing length (Pagonis et al., 2017).

424 Physical approaches to improving inlet response include inlet material substitution,

425 heating, and pressure reduction, to reduce adsorption of surface-active analytes through removal

426 of surface water and promoted mass transfer of analytes to the gas phase (Sintermann et al., 2011).

427 Deming et. al. (Deming et al., 2019) found that PFA tubing had the lowest delay times for

428 semivolatile compounds and would likely extend to small polar molecules like HCl. For a clean

429 thermally-equilibrated inlet, HCl artifacts can be minimized, but if semivolatile aerosol chloride is

430 sampled (e.g. NH_4Cl), the thermodynamic equilibrium can be shifted to result in a positive bias in

431 the HCl measurement, equivalent to similar considerations when measuring HNO_3 and NH_3 (Ellis

432 et al., 2010; Sintermann et al., 2011; Whitehead et al., 2008). While HEPA filters prevent aerosol

433 from entering the cavity, their elevated temperature (45 °C) could lead to volatilization bias and

434 therefore the use of an inlet filter held at ambient temperature to reduce such effects is

435 recommended at a minimum.

436 Chemical approaches can also help mitigate adsorption of surface-active molecules to inlet

437 surfaces through derivatization or passivation. The silanization of glass or stainless-steel to form

438   an inert fluorinated or silicon coating on a virtual impactor or the introduction of a gaseous

439   fluorinated compound that adsorbs competitively to instrument surfaces in place of the analytes

440   have been demonstrated to substantially reduce surface adsorption on PFA (Ellis et al., 2010;

441   Moravek et al., 2019; Pollack et al., 2019; Roscioli et al., 2016; Wilkerson et al., 2021). However,

442   environmental impacts must be considered when constantly adding fluorinated compounds to

443   sampling flows as they may have deleterious environmental consequences (Cousins et al., 2020).

444   In particular, perfluorobutanesulfonic acid, the fluorinated chemical suggested for passivating

445   inlets (Roscioli et al., 2016), is subject to usage restrictions in some European countries (ECHA,

446   2020) based on potential negative human and environmental health impacts (Benskin et al., 2012;

447   Sunderland et al., 2019). The high surface activity of perfluorobutanesulfonic acid is likely to cause

448   issues in the analyzer used in this work because the gas sample comes into direct contact with the

449   high reflectivity mirrors. Acid deposition onto mirrors will degrade their reflectivity. Silicon

450   coatings on all plumbed surfaces have been successfully used for atmospheric HCl measurements

451   (Wilkerson et al., 2021), and recommended for applications where PFA use is impractical.

452   Although a direct comparison has not been conducted for HCl, PFA inlet material has been

453   reported to yield better response times than silicon coatings for nitric acid (Neuman et al., 1999).

454   Differences in instrument configurations and applications may warrant the use of different inlet

455   materials and coatings for successful measurement of atmospheric HCl.

456   **Table 2.** Summary of the fit parameters for the double exponential decay curves as a
457   function of mixing ratio and humidity, e-folding response time, and t_{90}.
458

Mixing ratio (ppbv)	Residence time (seconds)	RH (%)	τ_1 (seconds)	τ_2 (seconds)	$1/e$ (seconds)	t_{90} (seconds)
12	0.021	0	10.3	123	26.5	101
16	0.028	0	9.6	200	24.7	82
21	0.037	0	10.1	300	26.4	74
24	–	0	2.7	97	2.5	10

		7	5.0	124	2.5	18
		14	5.0	114	2.5	32
		22	5.0	123	3.9	86
		33	10.0	189	16.1	239
32	0.056	0	9.4	188	24.5	62
45	0.079	0	9.7	350	25.6	54

4. Conclusions

The suitability of a CRDS analyzer for measuring ambient atmospheric HCl were explored through laboratory and ambient air intercomparisons, assessing their inlet and analyzer sampling challenges to established atmospheric sampling techniques for strong acids. In comparison to other reported instrumentation, the CRDS is shown performing similar or better than the most sensitive HCl measurements reported. As with many in situ measurements of HCl, the most significant limitation is adsorption/desorption loss and release on inlet surfaces, with the deposition effects increasing with increasing RH and decreasing HCl mixing ratios. Given the longstanding knowledge of these issues for surface active gases, such as HNO_3 and NH_3, there are a variety of chemical and physical options, discussed in this study, to mitigate inlet effects and achieve faster response times for the CRDS. Increasing the flowrate of the sampling inlet, while maintaining laminar flow, is the simplest approach to reducing surface effects discussed in Section 3.4. Spectra capturing errors in the measurement of HCl for the CRDS can occur at high levels of VOCs (e.g. near emission point sources or biomass burning plumes) or instrument instabilities (e.g. pressure fluctuations), however potential instrument errors are minimal under most operating and atmospheric conditions. Finally, comparison with annular denuder observations agreed within the combined uncertainties, with the CRDS measurement rate demonstrating the power of capturing transient events that are important to constraining atmospheric chlorine chemistry (e.g. photolysis of precursors, thermodynamic partitioning, and direct emissions).

Acknowledgements

We acknowledge the Natural Sciences Engineering and Research Council of Canada and York University for funding. We thank Andrea Angelucci and Sonya Daljeet for assistance with data collection.

References

Benskin, J. P., Muir, D. C. G., Scott, B. F., Spencer, C., De Silva, A. O., Kylin, H., Martin, J. W., Morris, A., Lohmann, R., Tomy, G., Rosenberg, B., Taniyasu, S. and Yamashita, N.: Perfluoroalkyl Acids in the Atlantic and Canadian Arctic Oceans, Environ Sci Technol, 46(11), 5815–5823, doi:10.1021/es300578x, 2012.

Bondy, A. L., Wang, B., Laskin, A., Craig, R. L., Nhliziyo, M. V, Bertman, S. B., Pratt, K. A., Shepson, P. B. and Ault, A. P.: Inland Sea Spray Aerosol Transport and Incomplete Chloride Depletion: Varying Degrees of Reactive Processing Observed during SOAS, Environ Sci Technol, (51), 9533–9542, doi:10.1021/acs.est.7b02085, 2017.

Butz, A., Dinger, A. S., Bobrowski, N., Kostinek, J., Fieber, L., Fischerkeller, C., Giuffrida, G. B., Hase, F., Klappenbach, F., Kuhn, J., Lübcke, P., Tirpitz, L. and Tu, Q.: Remote sensing of volcanic CO2, HF, HCl, SO2, and BrO in the downwind plume of Mt. Etna, Atmos Meas Tech, 10(1), 1–14, doi:10.5194/amt-10-1-2017, 2017.

Clegg, S. L. and Brimblecombe, P.: Potential degassing of hydrogen chloride from acidified sodium chloride droplets, Atmos Environ, 19(3), 465–470, doi:https://doi.org/10.1016/0004-6981(85)90167-2, 1985.

Cousins, I. T., Dewitt, J. C., Glüge, J., Goldenman, G., Herzke, D., Lohmann, R., Ng, C. A., Scheringer, M. and Wang, Z.: The high persistence of PFAS is sufficient for their management as a chemical class, Environ Sci Process Impacts, 22(12), 2307–2312, doi:10.1039/d0em00355g, 2020.

Crisp, T. A., Lerner, B. M., Williams, E. J., Quinn, P. K., Bates, T. S. and Bertram, T. H.: Observations of gas phase hydrochloric acid in the polluted marine boundary layer, J Geophys Res, 119, 6897–6915, doi:10.1002/2013JD020992, 2014.

Crosson, E. R.: A cavity ring-down analyzer for measuring atmospheric levels of methane, carbon dioxide, and water vapor, Appl Phys B Lasers Opt, 92(3), 403–408, doi:10.1007/s00340-008-3135-y, 2008.

Dawe, K. E. R., Furlani, T. C., Kowal, S. F., Kahan, T. F., Vandenboer, T. C. and Young, C. J.: Formation and emission of hydrogen chloride in indoor air, , 29, 70–78, doi:10.1111/ina.12509, 2019.

Deming, B. L., Pagonis, D., Liu, X., Day, D. A., Talukdar, R., Krechmer, J. E., Gouw, J. A. De, Jimenez, J. L. and Ziemann, P. J.: Measurements of delays of gas-phase compounds in a wide

515 variety of tubing materials due to gas – wall interactions, , (1), 3453–3461, 2019.

516 ECHA: Four new substances added to Candidate List, 2020.

517 Eisele, F. L. and Tanner, D. J.: Measurement of the gas phase concentration of H2SO4 and
518 methane sulfonic acid and estimates of H2SO4 production and loss in the atmosphere, J Geophys
519 Res Atmos, 98(D5), 9001–9010, doi:10.1029/93JD00031, 1993.

520 Ellis, R. a, Murphy, J. G., Pattey, E., Haarlem, R. Van and Brien, J. M. O.: Characterizing a
521 Quantum Cascade Tunable Infrared Laser Di ff erential Absorption Spectrometer (QC-TILDAS
522 ) for measurements of atmospheric ammonia, Atmos. Meas. Tech., 3309–3338, 2010.

523 Finlayson-Pitts, B. J., Ezell, M. J. and Pitts Jr., J. N.: Formation of chemically active chlorine
524 compounds by reactions of atmospheric NaCl particles with gaseous N2O5 and ClONO2,
525 Nature, 337(6204), 241–244, 1989.

526 Gard, E. E., Kleeman, M. J., Gross, D. S., Hughes, L. S., Allen, J. O., Morrical, B. D.,
527 Fergenson, D. P., Dienes, T., Ga, M. E., Johnson, R. J., Cass, G. R. and Prather, K. A.: Direct
528 Observation of Heterogeneous Chemistry in the Atmosphere, , 279(February), 1998.

529 Gordon, I. E., Rothman, L. S., Hill, C., Kochanov, R. V, Tan, Y., Bernath, P. F., Birk, M.,
530 Boudon, V., Campargue, A., Chance, K. V, Drouin, B. J., Flaud, J.-M., Gamache, R. R., Hodges,
531 J. T., Jacquemart, D., Perevalov, V. I., Perrin, A., Shine, K. P., Smith, M.-A. H., Tennyson, J.,
532 Toon, G. C., Tran, H., Tyuterev, V. G., Barbe, A., Császár, A. G., Devi, V. M., Furtenbacher, T.,
533 Harrison, J. J., Hartmann, J.-M., Jolly, A., Johnson, T. J., Karman, T., Kleiner, I., Kyuberis, A.
534 A., Loos, J., Lyulin, O. M., Massie, S. T., Mikhailenko, S. N., Moazzen-Ahmadi, N., Müller, H.
535 S. P., Naumenko, O. V, Nikitin, A. V, Polyansky, O. L., Rey, M., Rotger, M., Sharpe, S. W.,
536 Sung, K., Starikova, E., Tashkun, S. A., Auwera, J. Vander, Wagner, G., Wilzewski, J., Wcisło,
537 P., Yu, S. and Zak, E. J.: The HITRAN2016 molecular spectroscopic database, J Quant
538 Spectrosc Radiat Transf, 203, 3–69, doi:https://doi.org/10.1016/j.jqsrt.2017.06.038, 2017.

539 Hagen, C. L., Lee, B. C., Franka, I. S., Rath, J. L., Vandenboer, T. C., Roberts, J. M., Brown, S.
540 S. and Yalin, A. P.: Cavity ring-down spectroscopy sensor for detection of hydrogen chloride,
541 Atmos Meas Tech, 7(2), 345–357, doi:10.5194/amt-7-345-2014, 2014.

542 Haskins, J. D., Jaeglé, L., Shah, V., Lee, B. H., Lopez-Hilfiker, F. D., Campuzano-Jost, P.,
543 Schroder, J. C., Day, D. A., Guo, H., Sullivan, A. P., Weber, R., Dibb, J., Campos, T., Jimenez,
544 J. L., Brown, S. S. and Thornton, J. A.: Wintertime gas-particle partitioning and speciation of
545 inorganic chlorine in the lower troposphere over the northeast United States and coastal ocean, J
546 Geophys Res Atmos, 123(22), 12,897-12,916, doi:10.1029/2018JD028786, 2018.

547 Huey, L. G., Villalta, P. W., Dunlea, E. J., Hanson, D. R. and Howard, C. J.: Reactions of CF3O-
548 with atmospheric trace gases, J Phys Chem, 100, 190–194, doi:10.1021/jp951928u, 1996.

549 Jurkat, T., Voigt, C., Arnold, F., Schlager, H., Aufmhoff, H., Schmale, J., Schneider, J.,
550 Lichtenstern, M. and Dörnbrack, A.: Airborne stratospheric ITCIMS measurements of SO2, HCl,
551 and HNO3 in the aged plume of volcano Kasatochi, J Geophys Res Atmos, 115(D2),
552 doi:https://doi.org/10.1029/2010JD013890, 2010.

553 Karellas, N. S., Chen, Q. F., De Brou, G. B. and Milburn, R. K.: Real time air monitoring of
554 hydrogen chloride and chlorine gas during a chemical fire, J Hazard Mater, 102(1), 105–120,

555   doi:https://doi.org/10.1016/S0304-3894(03)00205-X, 2003.

556   Keene, W. C., Khalil, M. A. K., Erickson, D. J., McCulloch, A., Graedel, T. E., Lobert, J. M.,
557   Aucott, M. L., Gong, S. L., Harper, D. B., Kleiman, G., Midgley, P., Moore, R. M., Seuzaret, C.,
558   Sturges, W. T., Benkovitz, C. M., Koropalov, V., Barrie, L. A. and Li, Y. F.: Composite global
559   emissions of reactive chlorine from anthropogenic and natural sources: Reactive chlorine
560   emissions inventory, J Geophys Res, 104, 8429–8440, 1999.

561   Keene, W. C., Stutz, J., Pszenny, A. A. P., Maben, J. R., Fischer, E. V., Smith, A. M., von
562   Glasow, R., Pechtl, S., Sive, B. C. and Varner, R. K.: Inorganic chlorine and bromine in coastal
563   New England air during summer, J Geophys Res Atmos, 112(10), 1–15,
564   doi:10.1029/2006JD007689, 2007.

565   Keene, W. C., Long, M. S., Pszenny, A. A. P., Sander, R., Maben, J. R., Wall, A. J., O'Halloran,
566   T. L., Kerkweg, A., Fischer, E. V and Schrems, O.: Latitudinal variation in the multiphase
567   chemical processing of inorganic halogens and related species over the eastern North and South
568   Atlantic Oceans, Atmos Chem Phys, 9(19), 7361–7385, doi:10.5194/acp-9-7361-2009, 2009.

569   Kim, S., Huey, L. G., Stickel, R. E., Pierce, R. B., Chen, G., Avery, M. A., Dibb, J. E., Diskin,
570   G. S., Sachse, G. W., McNaughton, C. S., Clarke, A. D., Anderson, B. E. and Blake, D. R.:
571   Airborne Measurements of HCl from the Marine Boundary Layer to the Lower Stratosphere over
572   the North Pacific Ocean during INTEX-B, Atmos. Chem. Phys. Discuss., 8, 3563–3595, 2008.

573   Kochanov, R. V, Gordon, I. E., Rothman, L. S., Shine, K. P., Sharpe, S. W., Johnson, T. J.,
574   Wallington, T. J., Harrison, J. J., Bernath, P. F., Birk, M., Wagner, G., Le Bris, K., Bravo, I. and
575   Hill, C.: Infrared absorption cross-sections in HITRAN2016 and beyond: Expansion for climate,
576   environment, and atmospheric applications, J Quant Spectrosc Radiat Transf, 230, 172–221,
577   doi:https://doi.org/10.1016/j.jqsrt.2019.04.001, 2019.

578   Lao, M., R. Crilley, L., Salehpoor, L., C. Furlani, T., Bourgeois, I., Andrew Neuman, J., W.
579   Rollins, A., R. Veres, P., A. Washenfelder, R., C. Womack, C., J. Young, C. and C. Vandenboer,
580   T.: A portable, robust, stable, and tunable calibration source for gas-phase nitrous acid (HONO),
581   Atmos Meas Tech, 13(11), 5873–5890, doi:10.5194/amt-13-5873-2020, 2020.

582   Lee, B. H., Lopez-Hilfiker, F. D., Schroder, J. C., Campuzano-Jost, P., Jimenez, J. L., McDuffie,
583   E. E., Fibiger, D. L., Veres, P. R., Brown, S. S., Campos, T. L., Weinheimer, A. J., Flocke, F. F.,
584   Norris, G., O'Mara, K., Green, J. R., Fiddler, M. N., Bililign, S., Shah, V., Jaeglé, L. and
585   Thornton, J. A.: Airborne Observations of Reactive Inorganic Chlorine and Bromine Species in
586   the Exhaust of Coal-Fired Power Plants, J Geophys Res Atmos, 123(19), 11,225-11,237,
587   doi:10.1029/2018JD029284, 2018.

588   Ma, Y., He, Y., Yu, X., Chen, C., Sun, R. and Tittel, F. K.: HCl ppb-level detection based on
589   QEPAS sensor using a low resonance frequency quartz tuning fork, Sensors Actuators, B Chem,
590   233, 388–393, doi:10.1016/j.snb.2016.04.114, 2016.

591   MacInnis, J. J., VandenBoer, T. C. and Young, C. J.: Development of a gas phase source for
592   perfluoroalkyl acids to examine atmospheric sampling methods, Analyst, 141, 3765–3775,
593   doi:10.1039/C6AN00313C, 2016.

594   Marcy, T. P., Fahey, D. W., Gao, R. S., Popp, P. J., Richard, E. C., Thompson, T. L., Rosenlof,
595   K. H., Ray, E. A., Salawitch, R. J., Atherton, C. S., Bergmann, D. J., Ridley, B. A., Weinheimer,

A. J., Loewenstein, M., Weinstock, E. M. and Mahoney, M. J.: Quantifying Stratospheric Ozone in the Upper Troposphere with in Situ Measurements of HCl, Science (80-), 304(5668), 261 LP – 265, doi:10.1126/science.1093418, 2004.

Mattila, J. M., Lakey, P. S. J., Shiraiwa, M., Wang, C., Abbatt, J. P. D., Arata, C., Goldstein, A. H., Ampollini, L., Katz, E. F., Decarlo, P. F., Zhou, S., Kahan, T. F., Cardoso-saldan, F. J., Ruiz, L. H., Abeleira, A., Boedicker, E. K., Vance, M. E. and Farmer, D. K.: Multiphase chemistry controls inorganic chlorinated and nitrogenated compounds in indoor air during bleach cleaning, Environ Sci Technol, 54, 1730–1739, doi:10.1021/acs.est.9b05767, 2020.

Moravek, A., Singh, S., Pattey, E., Pelletier, L. and Murphy, J.: Measurements and quality control of ammonia eddy covariance fluxes: a new strategy for high-frequency attenuation correction, Atmos Meas Tech, 12, 6059–6078, doi:10.5194/amt-12-6059-2019, 2019.

Neuman, J. A., Huey, L. G., Ryerson, T. B. and Fahey, D. W.: Study of Inlet Materials for Sampling Atmospheric Nitric Acid, Environ Sci Technol, 33(7), 1133–1136, doi:10.1021/es980767f, 1999.

Osthoff, H. D., Roberts, J. M., Ravishankara, A. R., Williams, E. J., Lerner, B. M., Sommariva, R., Bates, T. S., Coffman, D., Quinn, P. K., Dibb, J. E., Stark, H., Burkholder, J. B., Talukdar, R. K., Meagher, J., Fehsenfeld, F. C. and Brown, S. S.: High levels of nitryl chloride in the polluted subtropical marine boundary layer, Nat Geosci, 1(5), 324–328, 2008.

Pagonis, D., Krechmer, J. E., de Gouw, J., Jimenez, J. L. and Ziemann, P. J.: Effects of gas–wall partitioning in Teflon tubing and instrumentation on time-resolved measurements of gas-phase organic compounds, Atmos. Meas. Tech., 10(12), 4687–4696, doi:10.5194/amt-10-4687-2017, 2017.

Place, B. K., Young, C. J., Ziegler, S. E., Edwards, K. A., Salehpoor, L. and VandenBoer, T. C.: Passive sampling capabilities for ultra-trace quantitation of atmospheric nitric acid (HNO3) in remote environments, Atmos Environ, 191(November 2017), 360–369, doi:10.1016/j.atmosenv.2018.08.030, 2018.

Pollack, I. B., Lindaas, J., Roscioli, J. R., Agnese, M., Permar, W., Hu, L. and Fischer, E. V: Evaluation of ambient ammonia measurements from a research aircraft using a closed-path QC-TILDAS operated with active continuous passivation, Atmos. Meas. Tech., 12(7), 3717–3742, doi:10.5194/amt-12-3717-2019, 2019.

Pszenny, A. A. P., Keene, W. C., Jacob, D. J., Fan, S., Maben, J. R., Zetwo, M. P., Springer-Young, M. and Galloway, J. N.: Evidence of inorganic chlorine gases other than hydrogen chloride in marine surface air, Geophys Res Lett, 20(8), 699–702, 1993.

Roberts, J. M., Osthoff, H. D., Brown, S. S. and Ravishankara, A. R.: N2O5 oxidizes chloride to Cl2 in acidic atmospheric aerosol, Science (80-), 321(4), 10, 2008.

Roscioli, J. R., Zahniser, M. S., Nelson, D. D., Herndon, S. C. and Kolb, C. E.: New Approaches to Measuring Sticky Molecules: Improvement of Instrumental Response Times Using Active Passivation, J Phys Chem A, 120(9), 1347–1357, doi:10.1021/acs.jpca.5b04395, 2016.

Sherwen, T., Schmidt, J. A., Evans, M. J., Carpenter, L. J., Großmann, K., Eastham, S. D., Jacob, D. J., Dix, B., Koenig, T. K., Sinreich, R., Ortega, I., Volkamer, R., Saiz-Lopez, A., Prados-

Roman, C., Mahajan, A. S. and Ordóñez, C.: Global impacts of tropospheric halogens (Cl, Br, I) on oxidants and composition in GEOS-Chem, Atmos. Chem. Phys., 16(18), 12239–12271, doi:10.5194/acp-16-12239-2016, 2016.

Simpson, W. R., Glasow, R. Von, Riedel, K., Anderson, P., Ariya, P., Bottenheim, J., Burrows, J. and Carpenter, L. J.: Halogens and their role in polar boundary-layer ozone depletion, Atmos Chem Phys, 4375–4418, 2007.

Simpson, W. R., Brown, S. S., Saiz-Lopez, A., Thornton, J. A. and Von Glasow, R.: Tropospheric halogen chemistry: Sources, cycling, and impacts, Chem Rev, 115(10), 4035–4062, doi:10.1021/cr5006638, 2015.

Sintermann, J., Spirig, C., Jordan, A., Kuhn, U., Ammann, C. and Neftel, A.: Eddy covariance flux measurements of ammonia by high temperature chemical ionisation mass spectrometry, Atmos. Meas. Tech., 4(3), 599–616, doi:10.5194/amt-4-599-2011, 2011.

Solomon, S.: Stratospheric ozone depletion: A review of concepts and history, Rev Geophys, 37(3), 275–316, doi:10.1029/1999RG900008, 1999.

Sunderland, E. M., Hu, X. C., Dassuncao, C., Tokranov, A. K., Wagner, C. C. and Allen, J. G.: A review of the pathways of human exposure to poly- and perfluoroalkyl substances (PFASs) and present understanding of health effects, J Expo Sci Environ Epidemiol, 29(2), 131–147, doi:10.1038/s41370-018-0094-1, 2019.

Thaler, R. D., Mielke, L. H. and Osthoff, H. D.: Quantification of Nitryl Chloride at Part Per Trillion Mixing Ratios by Thermal Dissociation Cavity Ring-Down Spectroscopy, Anal Chem, 83(7), 2761–2766, doi:10.1021/ac200055z, 2011.

Thornton, J. A., Kercher, J. P., Riedel, T. P., Wagner, N. L., Cozic, J., Holloway, J. S., Dube, W. P., Wolfe, G. M., Quinn, P. K., Middlebrook, A. M., Alexander, B. and Brown, S. S.: A large atomic chlorine source inferred from mid-continental reactive nitrogen chemistry, Nature, 464(11), 271–274, doi:10.1038/nature08905, 2010.

United States Environmental Protection Agency: Compendium of Methods for the Determination of Inorganic Compounds in Ambient Air: Determination of reactive acidic and basic gases and strong acidity of atmospheric fine particles (<2.5 μm) (Compendium Method IO-4.2)., 1999.

Valach, R.: The origin of the gaseous form of natural atmospheric chlorine ', Tellus Ser B Chem Phys Meteorol, 1967.

Veres, P. R., Roberts, J. M., Warneke, C., Welsh-Bon, D., Zahniser, M., Herndon, S., Fall, R. and de Gouw, J.: Development of negative-ion proton-transfer chemical-ionization mass spectrometry (NI-PT-CIMS) for the measurement of gas-phase organic acids in the atmosphere, Int J Mass Spectrom, 274, 48–55, 2008.

Voss, P. B., Stimpfle, R. M., Cohen, R. C., Hanisco, T. F., Bonne, G. P., Perkins, K. K., Lanzendorf, E. J., Anderson, J. G., Salawitch, R. J., Webster, C. R., Scott, D. C., May, R. D., Wennberg, P. O., Newman, P. A., Lait, L. R., Elkins, J. W. and Bui, T. P.: Inorganic chlorine partitioning in the summer lower stratosphere: Modeled and measured [ClONO2]/[HCl] during POLARIS, J Geophys Res Atmos, 106(D2), 1713–1732, doi:https://doi.org/10.1029/2000JD900494, 2001.

Wang, X., Jacob, D. J., Eastham, S. D., Sulprizio, M. P., Zhu, L., Chen, Q., Alexander, B., Sherwen, T., Evans, M. J., Lee, B. H., Haskins, J. D., Lopez-Hilfiker, F. D., Thornton, J. A., Huey, G. L. and Liao, H.: The role of chlorine in global tropospheric chemistry, Atmos Chem Phys, 19(6), 3981–4003, doi:10.5194/acp-19-3981-2019, 2019.

Webster, C. R., May, R. D., Trimble, C. A., Chave, R. G. and Kendall, J.: Aircraft (ER-2) laser infrared absorption spectrometer (ALIAS) for in-situ stratospheric measurements of HCl, N2O, CH4, NO2, and HNO3, Appl Opt, 33(3), 454–472, doi:10.1364/AO.33.000454, 1994.

Whitehead, J. D., Twigg, M., Famulari, D., Nemitz, E., Sutton, M. A., Gallagher, M. W. and Fowler, D.: Evaluation of Laser Absorption Spectroscopic Techniques for Eddy Covariance Flux Measurements of Ammonia, Environ Sci Technol, 42(6), 2041–2046, doi:10.1021/es071596u, 2008.

Wilkerson, J., Sayres, D., Smith, J., Allen, N., Rivero, M., Greenberg, M., Martin, T. and Anderson, J.: In situ observations of stratospheric HCl using three-mirror integrated cavity output spectroscopy, Atmos Meas Tech, 14(5), 3597–3613, doi:10.5194/amt-14-3597-2021, 2021.

Young, A. H., Keene, W. C., Pszenny, A. A. P., Sander, R., Thornton, J. A., Riedel, T. P. and Maben, J. R.: Phase partitioning of souble trace gases with size-resolved aerosols in near-surface continental air over northern Colorado, USA, during winter, J Geophys Res, 118, 9414–9427, doi:10.1002/jgrd.50655, 2013.

Young, C. J., Washenfelder, R. A., Roberts, J. M., Mielke, L. H., Osthoff, H. D., Tsai, C., Pikelnaya, O., Stutz, J., Veres, P. R., Cochran, A. K., Vandenboer, T. C., Flynn, J., Grossberg, N., Haman, C. L., Lefer, B., Stark, H., Graus, M., De Gouw, J., Gilman, J. B., Kuster, W. C. and Brown, S. S.: Vertically resolved measurements of nighttime radical reservoirs in los angeles and their contribution to the urban radical budget, Environ Sci Technol, 46(20), doi:10.1021/es302206a, 2012.

Young, C. J., Washenfelder, R. A., Edwards, P. M., Parrish, D. D., Gilman, J. B., Kuster, W. C., Mielke, L. H., Osthoff, H. D., Tsai, C., Pikelnaya, O., Stutz, J., Veres, P. R., Roberts, J. M., Griffith, S., Dusanter, S., Stevens, P. S., Flynn, J., Grossberg, N., Lefer, B., Holloway, J. S., Peischl, J., Ryerson, T. B., Atlas, E. L., Blake, D. R. and Brown, S. S.: Chlorine as a primary radical: evaluation of methods to understand its role in initiation of oxidative cycles, Atmos Chem Phys, 14, 3427–3440, 2014.

Young, C. J., Zhou, S., Siegel, J. A. and Kahan, T. F.: Illuminating the dark side of indoor oxidants, Environ Sci Process Impacts, 21(8), 1229–1239, doi:10.1039/C9EM00111E, 2019.

Zahniser, M. S., Nelson, D. D., McManus, B., Kebabian, P. L., Lloyd, D., Fowler, D., Jenkinson, D. S., Monteith, J. L. and Unsworth, M. H.: Measurement of trace gas fluxes using tunable diode laser spectroscopy, Philos Trans R Soc London Ser A Phys Eng Sci, 351(1696), 371–382, doi:10.1098/rsta.1995.0040, 1995.